Suppression of vortex pinning by field component parallel to the superconducting plane in Bi2Sr2CaCu2O8

Nakaharai, S; Ishiguro, T; Watauchi, S; Shimoyama, J; Kishio, K

PHYSICAL REVIEW B VOLUME 61, NUMBER 5 1 FEBRUARY 2000-I

Suppression of vortex pinning by field component parallel to the superconducting plane in $Bi_2Sr_2CaCu_2O_8$

S. Nakaharai
Department of Physics, Kyoto University, Kyoto 606-8502, Japan

T. Ishiguro
Department of Physics, Kyoto University, Kyoto 606-8502, Japan
and CREST, Japan Science and Technology Corporation, Saitama 322-0012, Japan

S. Watauchi
Institute of Inorganic Synthesis, Yamanashi University, Kofu 400-8511, Japan

J. Shimoyama and K. Kishio
Department of Superconductivity, University of Tokyo, Tokyo 113-8656, Japan
(Received 19 July 1999)

The response of magnetic fluxoids nearly parallel to the superconducting plane of the layered superconductor $Bi_2Sr_2CaCu_2O_8$ has been investigated through the ac susceptibility measurement. The fluxoids respond diamagnetically due to pinning when they pierce the superconducting plane to form pancake vortices, but they are released due to melting and become mobile in the high field. The liberation is enhanced by approaching the parallel field direction by the effect of decoupling between planes and finally the vortex pinning is suppressed. The pinning of fluxoids with pancakes and releasing in relation to their lock-in state are presented.

The vortex state in two-dimensional (2D) superconductors has been investigated mostly with respect to magnetic fields applied orthogonal to the 2D planes ($H_\perp$), where Abrikosov (pancake) vortices with normal cores are formed on the superconducting (SC) layers. The behavior of the vortex state can be affected by the field component parallel to the SC plane ($H_\parallel$). Deviation from the anisotropic Ginzburg-Landau model was demonstrated by vortex solid melting characteristics.[1–3] Meanwhile, when the external dc field is oriented parallel to the layers, the magnetic fluxoids are confined within the insulating layers (locked-in). In a low-field region, they are described as Josephson vortices, around which SC shielding current circulates. Their movement in the direction perpendicular to the SC plane is restricted due to intrinsic pinning,[4] but it is rather free along the conducting plane.[5] By inclining the magnetic field (H) from the SC plane so that $H_\perp$ exceeds the lower critical field (H_{c1}), the fluxoids pierce the SC plane forming pancake vortices. As a result, the whole vortex takes on a staircase shape, which consists of alternatively connected pancake and Josephson vortices. In this case, the fluxoid motion is impeded due to the pinning of the pancake part at imperfections and to the formation of a pinned vortex solid. Corresponding to this, the ac susceptibility (χ) exhibits a diamagnetic behavior.[6] However, pancake vortices become movable when the intensity of $H_\perp$ exceeds a threshold value corresponding to a first-order phase transition due to melting,[7–9] which is also considered to be accompanied by a decoupling of pancake vortices between adjacent layers. As an effect of field component parallel to the conducting plane, Bulaevskii *et al.*[10] have claimed that the staircase vortices become unstable with increase of the flux density and decouple to form a combined lattice consisting of independent pancake and Josephson vortices.

In this paper, we show the effects of magnetic fields parallel to the SC plane on the dynamics of vortices. In a high

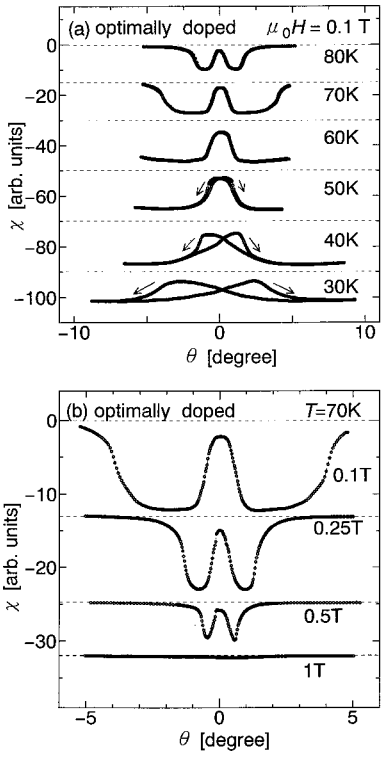

FIG. 1. (a) The ac susceptibility (χ) vs the tilt angle (θ) of the magnetic field from the SC plane under 0.1 T for an optimally doped sample. χ is presented in arbitrary units by shifting the base line. Arrows denote the direction of the angle sweep. (b) χ vs θ under different dc fields at $T=70$ K.

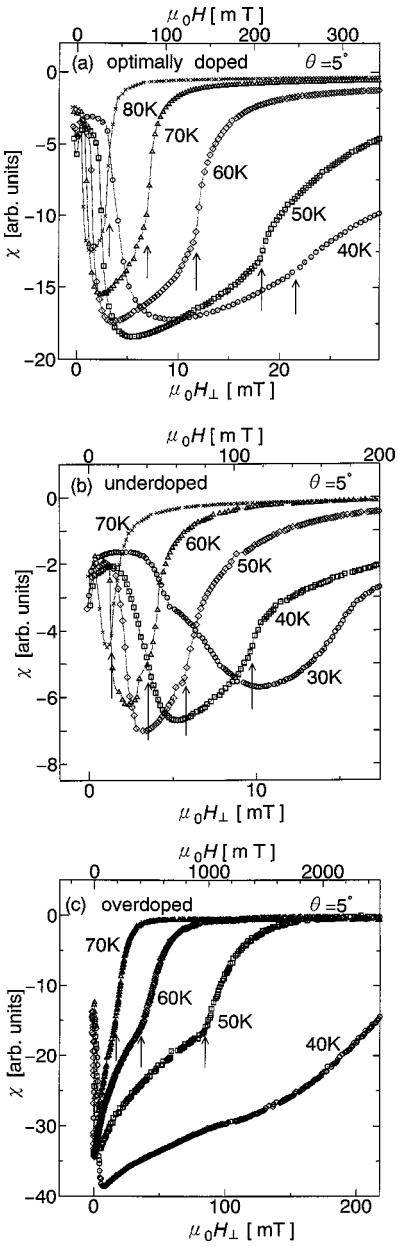

FIG. 2. Applied field dependence of χ for $\theta=5°$. Results for (a) optimally doped, (b) underdoped, (c) overdoped crystals are presented. The lower horizontal axis represents the field component perpendicular to the SC plane ($H_\perp$), while the upper horizontal axis represents the applied field value (H). A characteristic kink field ($H_\perp^*$, see text) is indicated by an arrow.

magnetic field, the flux pierces the SC planes even at a slight tilt angle. In this case, pancake vortices in adjacent layers are decoupled, and their dynamics can be represented by those for a 2D plane. We investigate the crossover between the pinned staircase vortex and the decoupled one from the viewpoint of the dynamics of fluxoids nearly along the conducting plane.

We used a floating-zone method to prepare $Bi_2Sr_2CaCu_2O_8$ samples with three different doping levels; underdoped, optimally doped, and overdoped crystals. Their SC transition temperatures (T_c) and anisotropy parameters (γ) were $T_c=88$ K and $\gamma=150$ for the optimally doped crystal, $T_c=77$ K and $\gamma=220$ for the underdoped crystal,

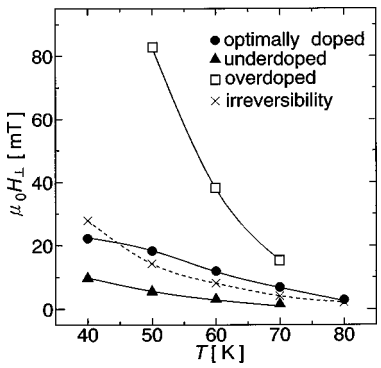

FIG. 3. The characteristic kink fields $H_\perp^*$ for optimally doped (closed circle), underdoped (closed triangle), and overdoped (open square) crystals are presented. The onset of the irreversibility field for the optimally doped crystal is indicated with cross marks in the figure. Lines are the guide to the eye.

$T_c=76$ K and $\gamma=90$ for the overdoped crystal. The size of the samples was $\sim 1.1\times 1.2\times 0.05$ mm^3. The ac susceptibility was evaluated by measuring the self-inductance of a coil containing $Bi_2Sr_2CaCu_2O_8$ single crystal. An LC resonance circuit consisting of the coil and a capacitor with a resonance frequency f was used in the frequency region of ~ 2 MHz. The self-inductance of the coil changed with the susceptibility of the crystal, and the frequency then shifted approximately as $\delta f \propto -\delta\chi$. The amplitude of the ac field was estimated to be ~ 1 μT. We set the coil axis to be parallel to the SC layer by sight. The coil and the sample were rotated together in a dc magnetic field.

Figure 1(a) shows χ as a function of a tilt angle (θ) for a dc field of 0.1 T, for the optimally doped $Bi_2Sr_2CaCu_2O_8$ crystal. The field was first increased from zero to 0.1 T at a large angle θ ($\sim 5°$ above 50 K, $\sim 10°$ below 40 K). Note that χ is represented in arbitrary units (corresponding to a shift of 100 Hz) by shifting the base line. At 80 K, with varying θ starting from $\theta=0$ (parallel field), the susceptibility first decreased and then returned to the starting value. As a result, χ exhibits two minima that is symmetric about the parallel field. Below 50 K, hysteresis was observed.

The central region, giving the local maximum in χ, was identified as a Josephson vortex lock-in region in which the vortices are movable along the layer. In this region, since the pinning of the Josephson vortex is considered to be weak, the penetration length of the ac field becomes long compared to the sample size and the vortices move freely as if the crystal was transparent.[6,11] The decrease in χ (diamagnetic response) due to the tilt is ascribed to the pinning of pancake vortices within the SC layer that causes a screening of the ac field. The relation between pinning and screening (diamagnetism) is described in Refs. 6, 12, and 13. Meanwhile, the recovery of the susceptibility at the higher θ can be understood in terms of a liberation from the pinning of pancakes, as will be described later. The angular dependence of the diamagnetic response at 70 K as a function of the field intensity is represented in Fig. 1(b). The angle region giving the diamagnetic response due to vortex pinning narrowed with the increase in H, and disappeared at 1 T.

In order to inspect the vortex dynamics from another aspect, $\chi(H)$ was obtained by setting $\theta=5°$. In this situation the length of the strings that connect the pancakes is con-

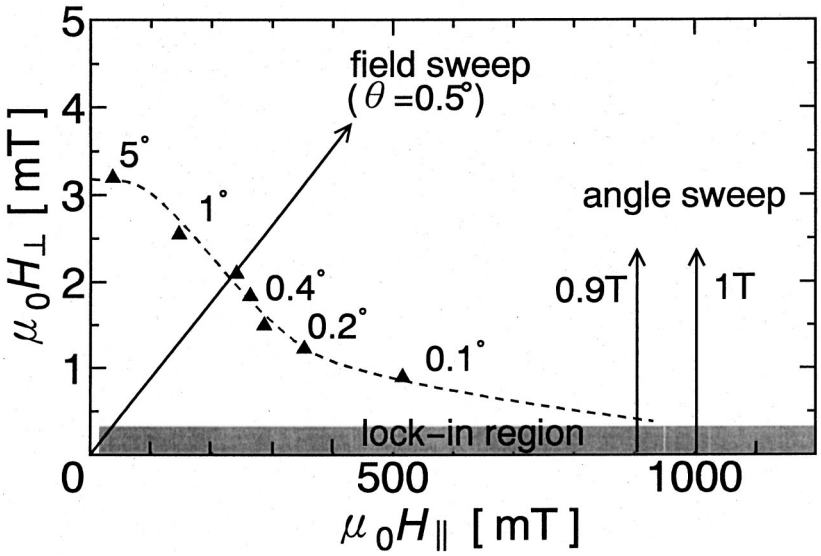

FIG. 4. An illustration of the $H_{\parallel}$ dependence of $H_{\perp}^{*}$ (closed triangles) in the $H_{\parallel}$-$H_{\perp}$ scheme for underdoped crystal at 60 K. The paths of field and angle sweep are displayed by long arrows. The upper bound field for the vortex solid state ($H_{\parallel}^{cr}$) exists between two vertical arrows.

stant, irrespective of the fluxoid density. The results for the optimally doped crystal are shown in Fig. 2(a), where the lower horizontal axis represents $H_{\perp}$ and the upper horizontal axis represents H. The diamagnetic response increased sharply near $H_{\perp}=0$, and then decreased rapidly with a further increase in H. The onset field ($H_{\perp}^{*}$) of the rapid decrease in the diamagnetic response, indicated by arrows in the figure, increased with decrease in temperature (T). We found that the $H_{\perp}^{*}$ was at the same level as the reported critical field for the melting of the vortex solid,[9] which was measured under a magnetic field perpendicular to the plane. This indicates that the suppression of the diamagnetic effect is associated with the melting of the pancake vortex solid formed on the plane. A similar measurement was carried out for the underdoped [Fig. 2(b)] and overdoped crystals [Fig. 2(c)]. For the overdoped crystal, the diamagnetic signal intensity decreased rapidly with the field in the region between the minimum and the anomaly point [Fig. 2(c)], in contrast to the optimally doped and underdoped crystals, which showed different curvature in this region. It is noteworthy that a similar difference in $\chi(H)$ was found in organic layered superconductors between κ-$(ET)_2Cu[N(CN)_2]Br$ and κ-$(ET)_2Cu(NCS)_2$. The lower anisotropy parameter case for κ-$(ET)_2Cu[N(CN)_2]Br$,[13,14] exhibits the similar diamagnetic response to the overdoped crystal, while κ-$(ET)_2Cu(NCS)_2$ (Refs. 6 and 14) behaves like optimally doped or underdoped crystals.

The temperature dependence of $H_{\perp}^{*}$ is presented in Fig. 3. For the optimally doped crystal, we evaluated the irreversibility field by the dc magnetization measurement using a superconducting quantum interference device susceptometer under a magnetic field applied perpendicularly to the SC plane. The irreversibility field (shown with a broken line) clearly deviates from the values of $H_{\perp}^{*}$, indicating that $H_{\perp}^{*}$ is not related to the irreversibility threshold but could be related to the melting.[13,15]

In order to clarify the influence of $H_{\parallel}$ on the pinning further, the field dependence of the susceptibility at angles from 0.1° to 5° was measured for the underdoped crystal. The field was swept after the sample was heated above T_c and then cooled in a zero field. The sweep rate was 0.05 T/min. In this case, the $H_{\perp}^{*}$ value was evaluated from the intersection of two tangential lines for the diamagnetic response versus field. The value of $H_{\perp}^{*}$ decreased with the tilt angle. In Fig. 4, the vortex pinning threshold represented by $H_{\perp}^{*}$ against $H_{\parallel}$ is demonstrated for the underdoped crystal at 60 K. The lock-in region, evaluated based on the angular width of the flat part of the central peak in $\chi(\theta)$ (see Mansky *et al.*,[6]) is represented by a gray zone whose boundary is almost independent of $H_{\parallel}$. In the $H_{\perp}$ versus $H_{\parallel}$ scheme, the inclined arrow line illustrates the path of the field sweep with $\theta=0.5°$. The closed triangles denote $H_{\perp}^{*}$. The pinned vortex region, giving diamagnetic χ, is represented by the area surrounded by the $H_{\perp}^{*}$ line (indicated by a broken line) and the lock-in region. The result is consistent with the tilt angle (from the perpendicular direction) dependence of the melting field reported in Refs. 1–3. The vertical arrows in Fig. 4 illustrate the paths of the angle sweep. It is notable that $H_{\perp}^{*}$ approaches the lock-in region with the increase in $H_{\parallel}$ and eventually merges with this region. We evaluated the critical $H_{\parallel}$ for the existence of the pinned vortex through the θ dependence, as in Fig. 1(b), and denoted it as $H_{\parallel}^{cr}$. The $H_{\parallel}^{cr}$ is understood as a threshold for destruction of the staircase vortex. In Fig. 5, the lower and upper ends of the error bar for $H_{\parallel}^{cr}$ are given by the fields under which the twin-dip structure appears and disappears in the θ dependence, respectively.

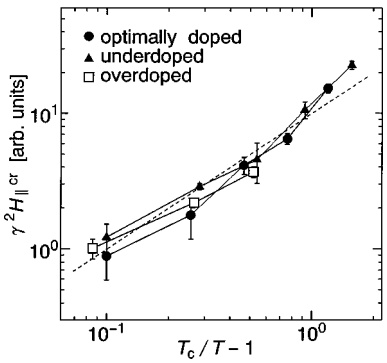

FIG. 5. Temperature dependence of $H_{\parallel}^{cr}$ for three crystals with different doping levels.

The plotted point is set at the midpoint of the error bar. We also investigated $H_{\parallel}^{\mathrm{cr}}$ for the optimally doped, underdoped, and overdoped crystals, and found that the T dependence of $H_{\parallel}^{\mathrm{cr}}$ for them can be scaled empirically as

$$H_{\parallel}^{\mathrm{cr}} \propto \gamma^{-2}(T_c/T-1), \tag{1}$$

as represented in Fig. 5, although the reason for this relation is open for study, where the deviation in the low-temperature side can be ascribed to the effect of the freezing as demonstrated by the hysteresis.

With the increase in $H_{\parallel}$ causing the decoupling,[10] pancake vortices are able to hop to neighboring Josephson strings, losing their connection with the strings. The probability increases with increases in the string density and the overlapping of Josephson vortices. In other words, the layers are decoupled with increases in $H_{\parallel}$, and the pancakes in the neighboring conducting plane tend to lose interlayer correlation.[16,17] As a result, the pancake vortex system becomes genuinely 2D. The melting temperature is decreased and approaches to the 2D limit T_m^{2D}, which is estimated to be 30–40 K for the optimally doped crystals[7] and independent of the field intensity. This is consistent with the disappearance of the pinned vortex solid in the high $H_{\parallel}$ region.

The authors are grateful to R. Ikeda for enlightening discussion. This work was supported by a grant for CREST from Japan Science and Technology Corporation. One of the authors (S.N.) acknowledges the Japan Society for Promotion of Science for their support.

[1] Y. Yamaguchi, H. Tomono, F. Iga, and Y. Nishihara, Physica C **273**, 261 (1997).
[2] B. Schmidt, M. Konczykowski, N. Morozov, and E. Zeldov, Phys. Rev. B **55**, R8705 (1997).
[3] S. Ooi, T. Tamegai, and T. Shibauchi, Physica C **282-287**, 1965 (1997).
[4] M. Tachiki and S. Takahashi, Solid State Commun. **70**, 291 (1989).
[5] H. Haneda, T. Ishiguro, S. Watauchi, J. Shimoyama, and K. Kishio, J. Phys. Soc. Jpn. **67**, 1391 (1998).
[6] P. A. Mansky, P. M. Chaikin, and R. C. Haddon, Phys. Rev. Lett. **70**, 1323 (1993).
[7] L. I. Glazman and A. E. Koshelev, Phys. Rev. B **43**, 2835 (1991).
[8] A. Houghton, R. A. Pelcovits, and A. Sudbø, Phys. Rev. B **40**, 6763 (1989).
[9] E. Zeldov, D. Majer, M. Konczykowski, V. B. Geshkenbein, V. M. Vinokur, and H. Shtrikman, Nature (London) **375**, 373 (1995).
[10] L. N. Bulaevskii, M. Ledvij, and V. G. Kogan, Phys. Rev. B **46**, 366 (1992).
[11] R. Ikeda and K. Isotani, J. Phys. Soc. Jpn. **68**, 599 (1999).
[12] M. W. Coffey and J. R. Clem, Phys. Rev. B **45**, 9872 (1992).
[13] N. H. Tea, F. A. B. Chaves, U. Klostermann, R. Giannetta, M. B. Salamon, J. M. Williams, H. H. Wang, and U. Geiser, Physica C **280**, 281 (1997).
[14] S. Nakaharai, T. Ishiguro, and G. Saito, J. Supercond. **12**, 579 (1999).
[15] T. Sasagawa, Y. Fujita, H. Kobayashi, J. Shimoyama, K. Kitazawa, and K. Kishio, Adv. Supercond. **XI**, 621 (1999).
[16] P. H. Kes, J. Aarts, V. M. Vinokur, and C. J. van der Beek, Phys. Rev. Lett. **64**, 1063 (1990).
[17] S. Theodorakis, Phys. Rev. B **42**, 10 172 (1990).